Mater.Phys.Mech.1 (2000) 15-19

HETEROEPITAXIAL GROWTH OF InAs ON Si: THE NEW TYPE OF QUANTUM DOTS

G.E. Cirlin[1,2], N.K. Polyakov[1,2], V.N. Petrov[1], V.A. Egorov[1], D.V. Denisov[2], B.V. Volovik[2], V.M. Ustinov[2], Zh.I. Alferov[2], N.N. Ledentsov[2,3], R. Heitz[3], D. Bimberg[3], N.D. Zakharov[4], P. Werner[4], U. Gösele[4]

[1] Institute for Analytical Instrumentation RAS, Rizhskiy pr. 26, 198103, St.Petersburg, Russia,
[2] A.F.Ioffe Physico-Technical Institute RAS, Polytechnicheskaya 26, 194021, St.Petersburg, Russia
[3] Technical University, Hardenbergstraße 36, 10623, Berlin, Germany
[4] Max-Plank-Institute for Microstructure Physics, Wecnberg 2, D-06120, Halle/Saale, Germany

Received: October 11, 1999

Abstract. Under certain growth conditions InAs/Si heteroepitaxial growth proceeds via Stranski-Krastanow or Volmer-Weber growth modes depending on the growth parameters. The critical thickness at which three dimensional InAs islands start to appear at the Si(100) surface is within the range of 0.7–4.0 monolayers (substrate temperature range is 350 °C – 430 °C). Their size depends critically on the growth conditions and is between 5 nm and 80 nm (uncapped islands). Critical lateral size of the coherent (Si capped) dislocation-free island is equal to 2–5 nm depending on the island height. Islands having larger size are dislocated. Optical properties of InAs nanoscale islands capped with Si reveal a luminescence band in the 1.3 μm region.

1. INTRODUCTION

Self-organisation effects on semiconductor surfaces which occure in the course of molecular beam epitaxy (MBE)have attracted much attention over the last ten years. A particular interest was shown in the quantum dots (QDs) in III/V – III/V(e.g., InAs – GaAs) [1, 2], II/VI – II/VI (e.g., CdSe – ZnSe) [3] or IV – IV (Si – Ge) [4] materials systems. This system stimulates much investigations because silicon remains a key material in the modern microelectronics industry. For optoelectronic applications silicon is not well suitable because of its indirect band gap nature. Attempts to improve the situation using SiGe – Si QDs did not lead to a significant progress as these nanostructures provide indirect band alignment both in k – and in real space. In order to increase luminescence efficiency of silicon-based structures we propose to insert direct bandgap InAs QDs in a Si matrix using MBE growth [5]. We emphasize that this approach is different from the growth utilizing InAs QDs on thick GaAs buffers [6]. Small coherent InAs islands additionally enable a possibility to overcome the problems of strong lattice mismatch and formation of antiphase domains inherent for the growth of thick III – V epilayers (e.g. GaAs) on Si.

In this paper we report on the MBE growth and properties of the InAs nanoscale islands formed on silicon. We have found that under certain growth conditions InAs/Si heteroepitaxial growth proceeds via Stranski-Krastanow or Volmer-Weber growth modes depending on the growth parameters leading to the formation of nanoscale islands. The lateral size depends critically on the growth conditions and is in the range of 2–80 nm. Optical properties of InAs QDs capped with Si reveal a luminescence band in the 1.3 μm region. A pronounced excitation density dependence of the photoluminescence (PL) peak position and a decay time of approximitely 400 ns were observed.

2. EXPERIMENTAL DETAILS

The growth experiments were carried out using EP1203 (Russia) or Riber Supra (France) MBE machines on exactly oriented Si(100) substrates. The Si(100) surface was prepared in a way similar to that described in [7]. Thermal desorption of silicon native oxide was performed in a growth chamber at the substrate temperature of 830 °C – 870 °C during 15 min. Afterwords, well-resolved (2×1) or mixed (1×2) and (2×1) surface reconstructions typical for cleaved Si(100) surface were observed. Then the substrate temperature was smoothly reduced to the desired value and the InAs deposition was initiated at a conventional MBE mode. The InAs deposition rate was typically 0.1 monolayer (ML) per

Corresponding author: G.E. Cirlin, e-mail: cirlin@beam.ioffe.rssi.ru

© 2000 Advanced Study Center Co. Ltd.

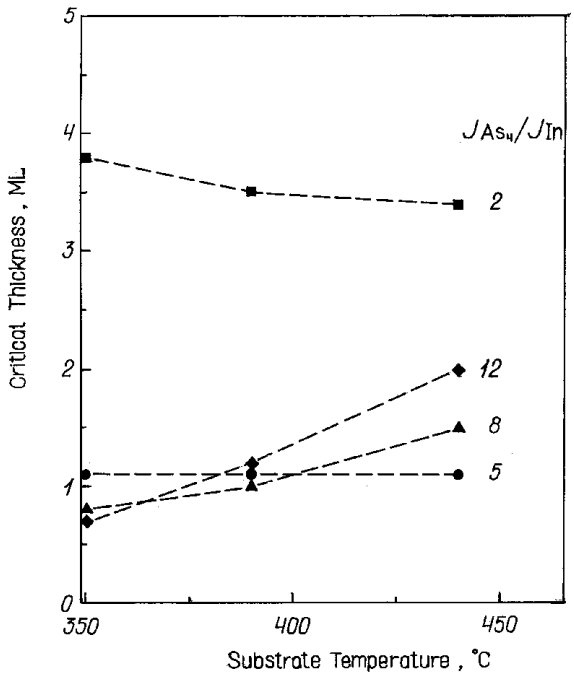

Fig. 1. Critical thickness dependence on substrate temperature and J_{As_4}/J_{In} fluxes ratio during InAs/Si growth.

second. When the deposition of the desired average thickness of InAs had been completed, the sample was immediately quenched to the room temperature and removed from the growth chamber in order to perform scanning tunnelling microscopy (STM) and scanning electron microscopy (SEM) studies. SEM measurements were performed using CamScan setup. Pieces for STM studies were covered with silicon vacuum oil immediately after exposure to the atmosphere, a procedure used before in our studies of InAs QDs on GaAs surfaces [8]. A calibration of the growth rate, III – V flux ratio, and monitoring of the surface morphology during growth was performed using reflection high energy electron diffraction (RHEED) system composed of a high sensitivity video camera, a video tape recorder and a computer, all interconnected via specially-designed interface [9]. Transmission electron microscopy (TEM) images were obtained on the samples when InAs islands were covered with 30–50 nm of silicon using JEOL 4000EX microscope. The same structures were used for luminescence experiments. A 514.5 nm line of the Ar^+ laser was used as an excitation source and a Ge photodiode as a detector. The excitation density was 5–100 W/cm^2. The structures for TEM and PL studies were grown in a following manner. Just after InAs deposition, a 10–20 nm Si cap layer was grown at the same substrate temperature T_s as for InAs deposition followed by a 10 min annealing procedure at 650 °C – 700 °C. Then 20–40 nm of Si was grown at the same temperature with optional consequent 10 min annealing at 700 °C – 800 °C in order to smooth the resulting surface.

3. RESULTS AND DISCUSSION

In Fig.1 we summarise RHEED data of the dependencies of the substrate temperatures and As_4/In fluxes ratio in the ranges 350 °C – 450 °C and 2 – 12, respectively, on the critical thickness d_{crit} (mean thickness at which 3D nanoscale islands start to appear at the surface). The lowest limit of T_s was chosen for two reasons: first, determination of T_s at very low temperatures is difficult and second, because of poor quality of Si cap layer grown at too low temperatures. Poor quality of the Si cap layer may hinder the device applications. On the other hand, we have found that at temperatures higher then 450 °C *no nanoislanding is observed on the surface* independently on the V/III flux ratio, total arsenic overpressure, *etc.* limiting the range for the highest T_s as indicated in Fig.1. (At higher T_s only mesoscopic dislocated clusters with lateral size of ~400 nm appeared on the Si(100) surface [10]). Following the data presented in Fig.1 one can conclude that depending on the growth conditions, 2D–3D transition can be tuned in the thickness range of 0.7–4.0 ML. On the other hand, we have observed two different growth modes for the InAs/Si heteroepitaxial growth. First, Volmer–Weber growth mechanism could be realised when InAs nanoscale islands are formed on the bare Si substrate (i.e. for d_{crit}<1 ML). Typical RHEED pattern for this case is presented in Fig. 2,a. At higher T_s (400 °C – 450 °C) we observed Stranski-Krastanow growth mechanism when d_{crit} exceeded 1.0 ML and the formation of InAs nanoscale islands occurs on the top of the wetting layer. RHEED pattern for this particular case is presented in Fig. 2,b. These results are in agreement with the 2D – 3D transition intervals observed by other groups [11, 12].

Typical surface morphology extracted from the STM images for these cases revealed high density arrays of nanoscale islands (with surface density of the order of $((1\div6)\times10^{11}$ cm^{-2}) and the lateral sizes of 10–20 nm [13, 14]. These islands are basically pyramidal in shape with rectangular or triangular base.

We have found that the growth conditions (the amount of InAs deposited, fluxes ratio influenced greatly the arrangement, sizes and surface density of InAs/Si islands [15]. In order to clarify how growth parameters influence the surface morphology we grew three samples, labelled 1–3. Their MBE growth conditions and geometrical characteristics measured with SEM are presented in the Table 1.

The main trends for the uncapped InAs/Si island formation are the following. At higher As pressure and

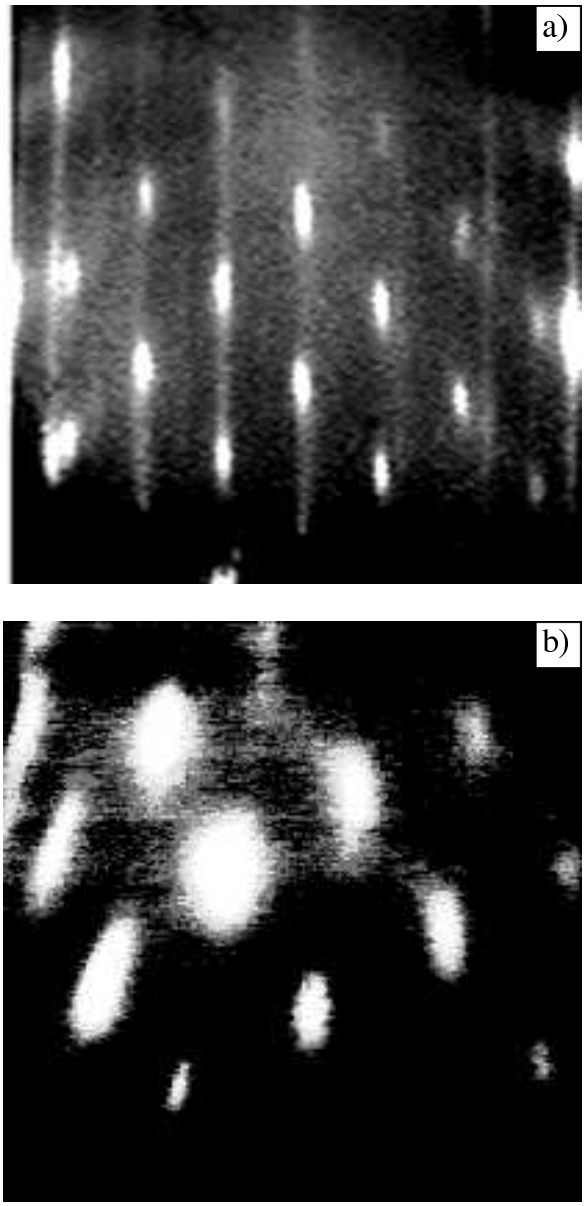

Fig. 2. Typical RHEED patterns in [011] direction taken after the formation of InAs 3D islands in Si(100) surface via (a) Volmer-Weber and (b) Stranski-Krastanow growth modes.

the same InAs mean thickness the island size drops as compared to the case of the decreased As/In fluxes ratio (samples 1 and 3). We believe that this is due to the suppressing of the surface migration length. The density of the islands for the sample 3 is four times higher than that of the sample 1. The islands size distribution becames narrower, too. With increasing the average InAs thickness (sample 2) the islands start to form large conglomerates. These clusters are elongated and exhibit crystallographic shape with the base oriented along [011] and [01$\bar{1}$] directions. The similar situation was observed in [11] where such clusters were formed during the InAs growth on Si(100) passivated (hydrogen-terminated) surfaces with approximately same size and surface density. We note that for the sample 2 the critical thickness is larger by the value of 1.8 ML, *i.e.* 2.5 times higher. In InAs/GaAs heteroepitaxial system such large sizes should lead to the formation of the dislocations. In order to check the crystalline quality we studied the same uncapped samples with cross—sectional TEM.

Most of the islands exhibited considerably good crystalline quality although misfit dislocations appeared at the InAs/Si interface. In Fig. 3 typical cross-section TEM image for single InAs nanoisland is presented. Using high resolution TEM data taken from the Si capped samples we have found that the critical lateral size of the coherent dislocation—free islands is equal to 2-5 nm depending on the island height. Islands of

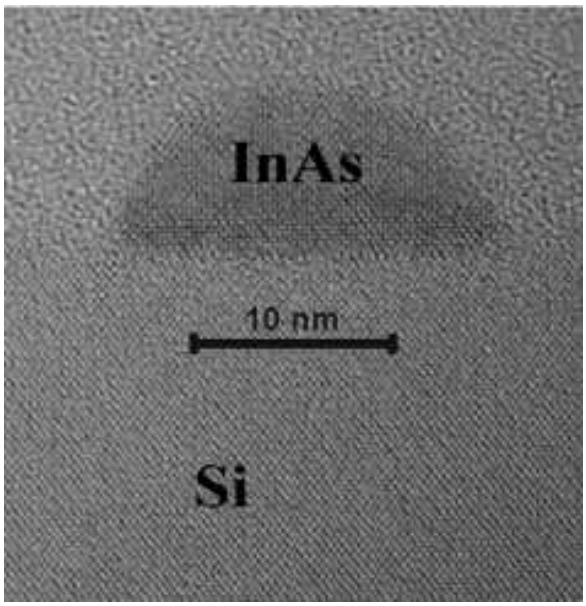

Fig. 3. Typical high resolution cross-section TEM image of the single InAs nanoscale island at Si(100) surface.

Table. MBE growth conditions and geometrical characteristics of the InAs/Si(100) quantum dot samples

Sample No.	*InAs thickness, ML*	*As/In fluxes ratio*	*Island lateral size, nm*	*Surface density of islands, 10^{10} cm^2*
1	1.2	3	15–50	4
2	2.5	3	20–80	1.6
3	1.2	10	3–15	16

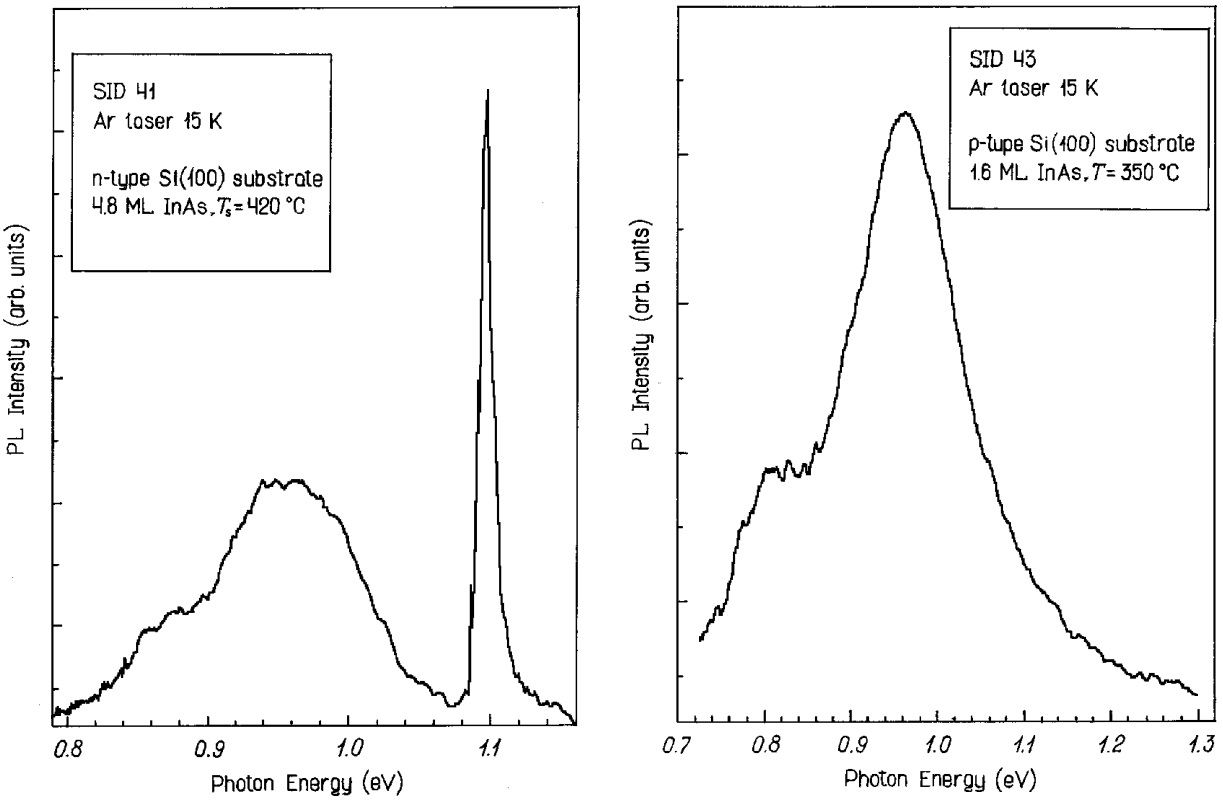

Fig. 4. PL data for the InAs nanostructures embedded in Si matrix: (a) InAs grown via Stranski-Krastanow, (b) InAs grown via Volmer-Weber growth modes.

larger size are defected due to misfit dislocations or twins. We also suggested that most of the InAs reevaporated during the deposition (or annealing) of the cap layer. Fig. 3. shows typical high resolution cross-section TEM image of the single InAs nanoscale island at Si(100) surface.

The samples with such InAs quantum dots capped with 30–50 nm Si layer show a luminescence band in the 1.3 μm region for temperatures up to ~170K. The PL exhibited a pronounced blue shift with increasing the excitation density and decays at the time constant of ~400 ns [16]. Fig.4 compares low temperature PL spectra of the 4.8 ML with the 1.6 ML InAs samples deposited in different growth modes (Stranski-Krastanow for 4.8 ML and Volmer-Weber for 1.6 ML*. These spectra reveal TO-phonon assisted exciton emission of the Si substrate and barrier at ~1.11 eV. The broad emission band in the 0.9 to 1.05 eV region was observed for both InAs deposition thickness suggesting its origin to be associated with the InAs nanoobjects embedded in Si matrix. This broad line was not observed for the samples with InAs insertions smaller than the critical thickness or on a Si substrate. However, the size of these insertions evaluated using TEM measurements does not exceed 5 nm [16] which is definitely not enough for charge localisation and quantum confinement.

Our very recent detailed TEM investigation of these samples shows that besides a random distribution of InAs molecules, two kinds of ordering were detected. Such regions ($\phi < 6$ nm) are characterised by larger InAs concentration. The first kind shows an ordering of InAs molecules in (101), ($10\bar{1}$) planes inclined to the [001] growth direction, while in the second one the ordered (110), ($1\bar{1}0$) planes are parallel to the [001] growth direction. The formation of such a structure results in energy lowering due to the decrease of the number of mixed Si–As and Si–In bonds. We believe that the appearance of the broad PL peak is the result of solid solution formation and/or ordering, because the incorporation of InAs molecules into Si matrix changes the band gap of material and possibly shifts the relative positions of conduction and valence bands. Detailed results on TEM study will be presented in a separate paper [17].

4. CONCLUSIONS

We have demonstrated that InAs/Si(100) heteroepitaxial growth might proceed via Stranski - Krastanow or Volmer-Weber growth modes depending on the MBE growth parameters. Critical thickness at which three dimensional InAs islands start to ap-

* InAs critical thickness for both samples was exceeded by the value of 0.8 ML.

pear at the Si(100) surface varies within the range of 0.7–4.0 monolayers (substrate temperature is 350 °C – 430 °C, As/In fluxes ratio is 2–12). Their size depends critically on the growth conditions and is between 5 nm and 80 nm (uncapped islands). Critical lateral size for Si capped InAs coherent dislocation-free islands is equal to 2–5 nm depending on the island height. Islands of larger size are dislocated. Optical properties of the InAs nanoscale islands capped with Si reveal a luminescence band in the 1.3 μm region independently on the growth mode used for InAs deposition. The appearance of this peak can be caused by the solid solution formation and/or ordering due to the incorporation of InAs molecules into Si matrix during post growth annealing which changes the band gap of material and possibly shifts the relative positions of conduction and valence bands. InAs/Si heteroepitaxial system seems to be promising for Si–based optoelectronic applications, in particular for short distance fiber optics and integration of microelectronics and optical parts at the same silicon wafer.

ACKNOWLEDGEMENTS

The authors thanks to N.P. Korneeva, V.N. Demidov, S.A. Masalov and V.M. Busov for their kind assistance during experiments. This work was supported by INTAS Grant No. 96-0242, Russian Foundation for Basic Research Grant No. 98-02-18317 and Grant No. 99-02-16799, Russian Scientific Programmes "Physics of Solid State nanostructures" Grant No. 98-2029 and "Methods and Devices of Micro- and Nanoelectronics" Grant No 02.04.5.1.40.E.46.

REFERENCES

[1] L. Goldstein, F. Glas, J.Y. Marzin, M.N. Charasse, and G.Le Roux // *Appl.Phys.Lett.* **47** (1985) 1099.

[2] D. Leonard, M. Krishnamurthy, C.M. Reaves, S.P. Denbaars and P.M. Petroff // *Appl.Phys.Lett.* **63** (1993) 3203.

[3] M. Strassburg, V. Kutzer, U.W. Pohl, A. Hoffmann, I. Broser, N.N. Ledentsov, D. Bimberg, A. Rosenauer, U. Fischer, D. Gerthsen, I.L. Krestnikov, M.V. Maximov, P.S. Kop'ev and Zh.I. Alferov // *Appl. Phys. Lett.* **72** (1998) 942.

[4] Feng Liu and M.G.Lagally // *Surf. Sci.* **386** (1997) 169.

[5] N.N. Ledentsov in: Proceedings of the 23rd International Conference on the Physics of Semiconductors, Berlin, Germany, July 21-26, 1996, edited by M. Scheffler and R. Zimmermann (World Scientific, Singapoure, 1996) **1** p. 19.

[6] J.M. Gerard, O. Cabrol and B. Sermage // *Appl.Phys.Lett.* **68** (1996) 3123.

[7] A. Ishisaka and Y. Shiraki // *J. Electrochem. Soc.* **133** (1986) 666.

[8] G.E. Cirlin, G.M. Guryanov, A.O. Golubok, S.Ya. Tipissev, N.N. Ledentsov, P.S. Kop'ev, M. Grundmann and D. Bimberg // *Appl. Phys. Lett.* **67** (1995) 97.

[9] G.M. Gur'yanov, V.N. Demidov, N.P. Korneeva, V.N. Petrov, Yu.B. Samsonenko and G.E. Tsyrlin // *Tech. Phys.* **42** (1997) 956.

[10] G.E. Cirlin, V.N. Petrov, V.G. Dubrovskii, S.A. Masalov, A.O. Golubok, N.I. Komyak, N.N. Ledentsov, Zh.I. Alferov and D. Bimberg // *Tech. Phys. Lett.* **24** (1998) 290.

[11] T. Mano, H. Fujioka, K. Ono, Y. Watanabe and M. Oshima // *Appl. Surf. Sci.* **130—132** (1998) 760.

[12] P.C. Sharma, K.W. Alt, D.Y. Yeh and K.L. Wang // *Appl. Phys. Lett.* **75** (1999) 1273.

[13] G.E. Cirlin, V.G. Dubrovskii, V.N. Petrov, N.K. Polyakov, N.P. Korneeva, V.N. Demidov, A.O. Golubok, S.A. Masalov, D.V. Kurochkin, O.M. Gorbenko, N.I. Komyak, V.M. Ustinov, A.Yu. Egorov, A.R. Kovsh, M.V. Maximov, A.F. Tsatsul'nikov, B.V. Volovik, A.E. Zhukov, P.S. Kop'ev, Zh.I. Alferov, N.N. Ledentsov, M. Grundmann and D. Bimberg // Semicond. Sci. Technol. **13** (1998) 1262.

[14] G.E. Cirlin, V.N. Petrov, V.G. Dubrovskii, Yu.B. Samsonenko, N.K. Polyakov, A.O. Golubok, S.A. Masalov, N.I. Komyak, V.M. Ustinov, A.Yu. Egorov, A.R. Kovsh, M.V. Maximov, A.F. Tsatsul'nikov, B.V. Volovik, A.E. Zhukov, P.S. Kop'ev, N.N. Ledentsov, Zh.I. Alferov and D. Bimberg // *Semiconductors* **33** (1999) 972.

[15] G.E. Cirlin, N.K. Polyakov, V.N. Petrov, V.A. Egorov, Yu.B. Samsonenko, B.V. Denisov, V.M. Busov, B.V. Volovik, V.M. Ustinov, Zh.I. Alferov, N.N. Ledentsov, D. Bimberg, N.D. Zakharov and P. Werner // *Czeck. J. Phys.* **49** (1999) 1547.

[16] R. Heitz, N.N. Ledensov, D. Bimberg, A.Yu. Egorov, M.V. Maximov, V.M. Ustinov, A.E. Zhukov, Zh.I. Alferov, G.E. Cirlin, I.P. Soshnikov, N.D. Zakharov, P. Werner and U. Gösele // *Appl. Phys. Lett.* **74** (1999) 1701.

[17] N.D. Zakharov et.al., in: MRS'99 Fall meeting proceedings, in press.